CHAPTER 4

HIGH-QUALITY-FACTOR PARYLENE-C-BASED INTRAOCULAR PRESSURE SENSOR

4.1 Overview

Intraocular pressure (IOP) has been important information for the prevention and treatment of certain human eye diseases. For example, glaucoma is the second leading cause of blindness worldwide according to World Health Organization [6]. The majority of glaucoma patients have an IOP > 20 mmHg (compared to a normal IOP of ~ 10 mmHg), which could damage patients' optic nerves in the backside of the eye and cause the irreversible blindness. Currently, there is no cure for glaucoma, however, with early diagnosis and proper treatment, the visual loss can usually be slowed down or eliminated. Due to the lack of other symptoms or pain and the eye's ability to compensate for loss of peripheral vision, many glaucoma patients are unaware of the disease's development, until it is already severe. In fact, only half of the patients in the U.S are aware of having glaucoma. Therefore, early diagnosis and treatment are important to prevent blindness. Thus, a device to diagnose early-stage glaucoma is in demand.

As IOP is a convenient biomarker of glaucoma, it is generally measured in clinics to determine the presence of the disease. Current clinical IOP measurement is typically done with applanation tonometry. There are primarily two types of applanation

tonometers and both are non-implantable. The first type uses physical contact approach to touch the cornea and to estimate the area of the flattened portion. The IOP can then be calculated by the given applanation force and the flattened cornea area [155]. This approach requires well-trained ophthalmologists. The other type of applanation tonometers, named pneumotonometry, obtains the IOP by puffing an air jet onto the eye and measuring the flattened portion of the cornea optically [79]. Due to its non-contact characteristics and fine optical sensors, pneumotonometry can provide more accurate IOP information than the contact approach. However, the cornea's mechanical properties and thickness do vary from person to person, so the assumed cornea properties would always introduce errors. Interestingly, it's also reported that depending on daily activities, a person's IOP can actually go up to as high as 25 mmHg (i.e., above the glaucoma threshold IOP), while the IOP measured in clinic actually shows a normal value [84, 85, 156–158]. Therefore, the monitoring of a patient candidate's IOP should be 24/7 continuously. Unfortunately, current applanation tonometers, as clinical equipments, cannot provide this capability. Therefore, an implant sensor that can monitor the IOP continuously and wirelessly will be highly desirable [87].

Either active or passive approaches can be adopted to fulfill the telemetric pressure sensing [87]. Although the active devices are more likely to provide more functions, they tend to consume more power during the operation. Therefore power supply is a big issue. In addition, an active implant may require a significant size, which is of special concern for intraocular placement. However, with the infusion of MEMS (micro electro mechanical systems) technologies, miniaturized telemetric pressure sensors have already been developed for physiological pressure sensing applications such

as intracranial pressure monitoring by Leung [159]. For IOP measurement, Mclaren's IOP sensor had a commercial transducer implanted on the dorsal neck of the rabbit under test with a catheter going to the anterior chambers [88]. Mokwa's IOP sensor was designed to be implanted in the lens [89]. Leonardi built a thin-microfabricated platinum-titanium strain gauge on a soft contact lens which can be worn directly on the cornea [160]; Chow designed a tadpole-shaped IOP sensor and would curve along the rim of the anterior chamber after the device implantation [161].

As seen from the above examples, there could be many different approaches for active IOP sensing; however, in any case one must consider collectively the implant size, the placement and the corresponding surgical procedures because eye is a small and delicate organ, and has very limited room inside. Passive IOP sensors may have many advantages over active ones in terms of smaller size, little or no power consumption, and easier surgery. One especially interesting passive IOP approach is to use LC-tank-based sensors with a pressure–dependent capacitor and/or inductor. This approach has also been studied for decades and is well established [90, 92, 93, 162]. Different physiological pressure monitoring has been achieved using passive telemetry. For examples, DeHennis has adopted the technique to monitor the transcutaneous pressure [94]; Fonseca also utilized it for pressure monitoring of abdominal aortic aneurysms (AAA) [95]. For IOP implants, Collins published the first passive wireless transensor implantable in the anterior chamber in 1967 adopting the LC-tank resonant circuit to measure the IOP [91]. Backlund et al. modified Collins' IOP sensor design using a capacitive sensor manufactured by silicon fusion bonding technique [96, 163, 164]. The capacitor was connected to a hand-wound coil made of 50 μm gold wire to form a LC-

tank resonant circuit and the entire system was encapsulated by silicone for biocompatibility.

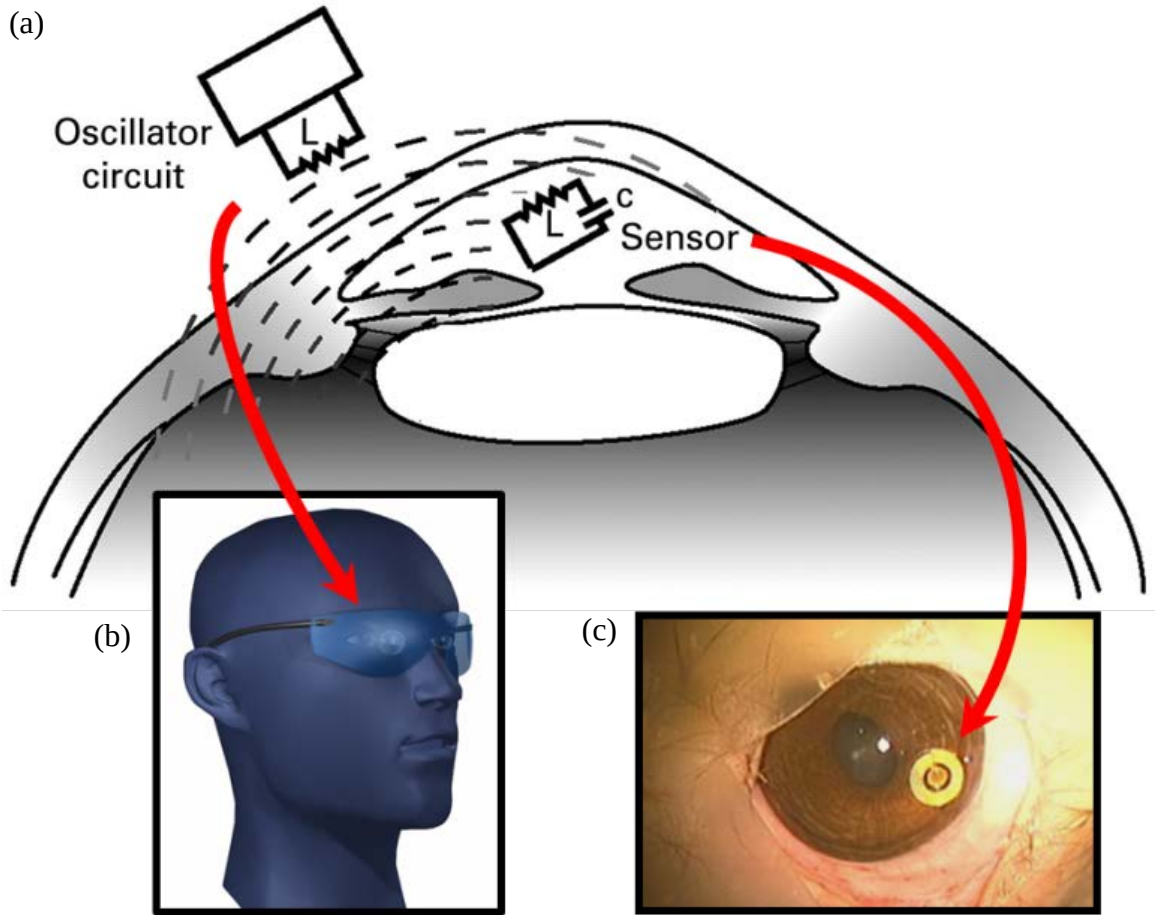

Figure 4-1: (a) Wireless sensing concept of implantable IOP sensor in the anterior chamber, (b) the glass reader paradigm, (c) a real IOP sensor *in vivo* tested in a rabbit eye

This work presents our effort to develop a telemetric implantable IOP sensor using an LC-tank resonant circuit. In fact, our group presented a flexible parylene-based IOP sensor by Chen et al. in 2010 [98]. The sensor had one inductor and one capacitor combined in series as a passive LC-tank resonance circuit. The IOP sensor was implanted into the anterior chamber and anchored on the iris, as shown in Figure 4-1(a).

Figure 4-1 (c) shows the *in vivo* test of Chen's IOP sensor in a rabbit eye. The resonant frequency shift was registered by an external oscillator circuit through a wireless inductive coupling link, whose concept is shown in Figure 4-2. The external interrogating circuit could be designed and even integrated into a pair of glasses as shown in Figure 4-1 (b). With the sensor's principle shown in Figure 4-3 (a), when the sensor's surrounding pressure increases, the capacitance increases due to the sensing plate's deforming concavely, introducing the resonant frequency shifts to the lower range.

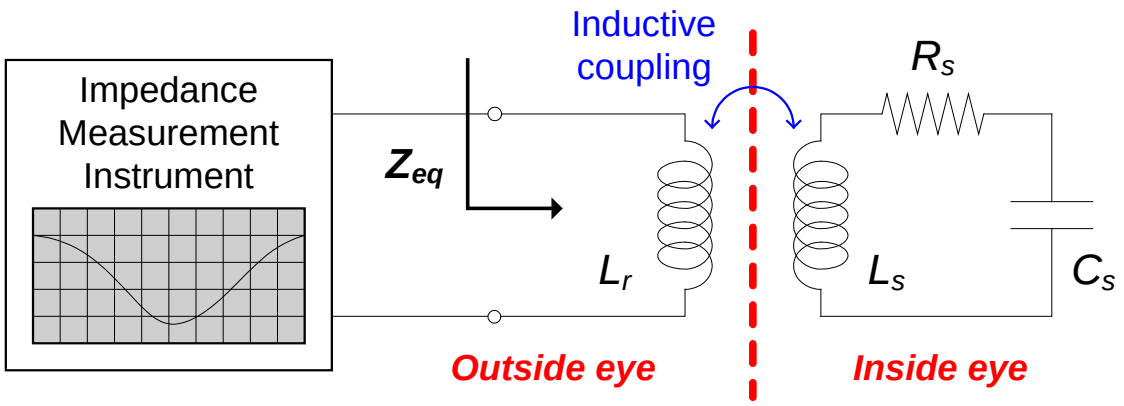

Figure 4-2: The concept of the wireless inductive coupling link: The frequency shift is registered through an external oil reader.

Although the IOP sensor could successfully measure the pressure information of the eye, the anchoring of the sensor was still an issue. In Chen's work, a modified iris retractor was attached to the bottom of the IOP sensor so that the sensor can anchor on top of the iris after the implantation. However, the iris would contract or expand very frequently and the iris retractor might get loose. In addition, due to the high loss tangent of the eye fluid in the anterior chamber, the LC tank's quality factor was degraded and

the sensing distance was reduced just as what have been reported in other wireless sensors [95, 97, 98].

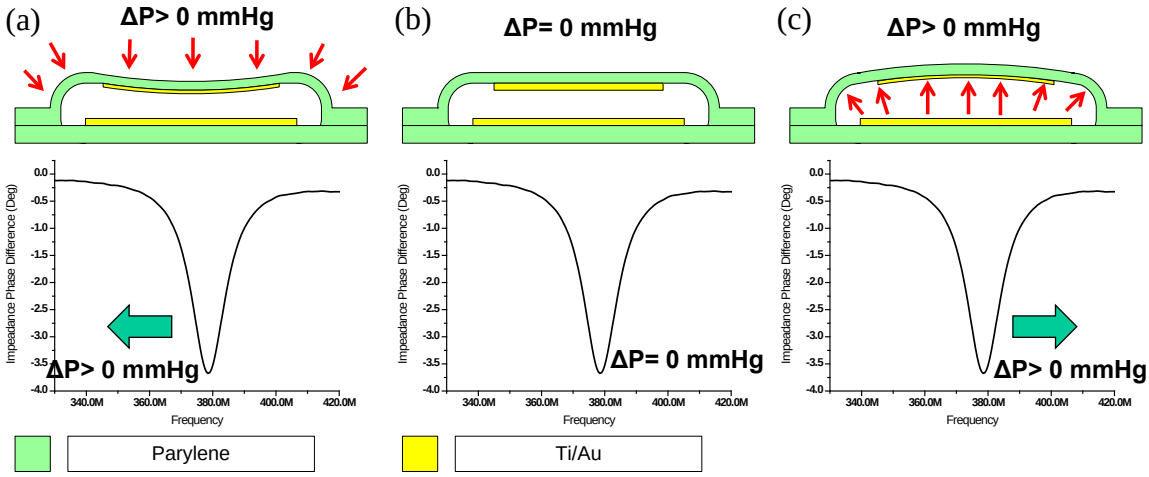

Figure 4-3: Resonant frequency shift corresponds to the applied pressure: (a) Frequency decreases as the capacitance increases; (b) No frequency shift is observed when no pressure difference exists; (c) Frequency increases as the capacitance decreases.

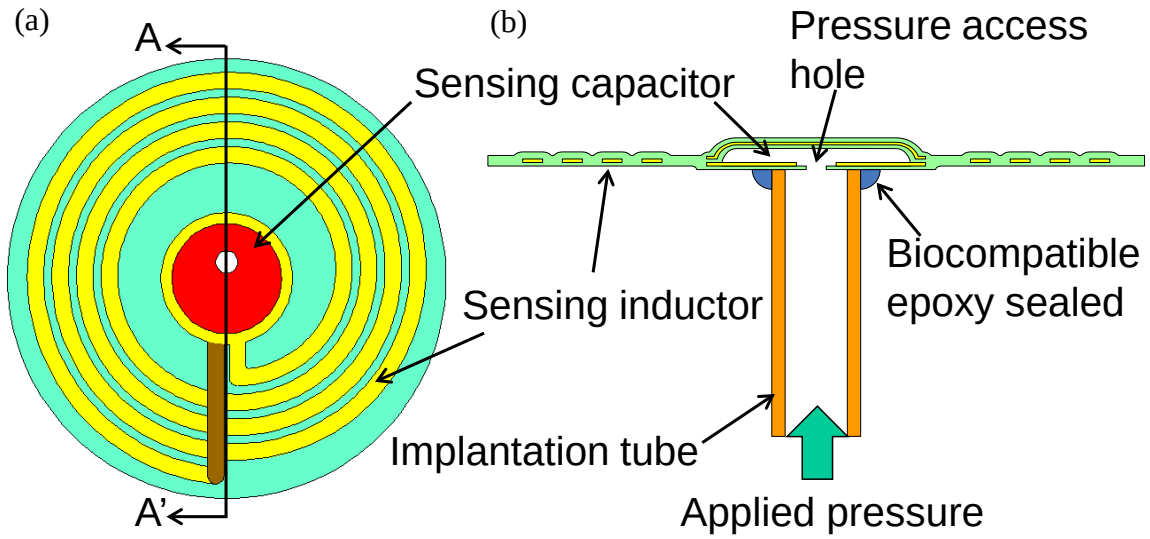

Figure 4-4: The new IOP sensor design: (a) Top view of the sensing part, (b) AA' cross-section view of the IOP sensor

To overcome these problems, a new IOP sensor structure is developed. We keep the sensing part design similar to our previous device, which is composed of a sensing inductor and a sensing capacitor as shown in Figure 4-4 (a). A pressure access hole connecting the chamber of the sensing capacitor and outside is created during device fabrication. The pressure access hole allows an implantation tube to be attached to the backside of the device to cover the access hole as shown in Figure 4-4 (b). During the device fabrication, a biocompatible epoxy is applied to seal the gap between the implantation tube and the sensing part to make it airtight, and also to ensure the device's biocompatibility.

The newly designed IOP sensor could be placed with an implantation tube penetrating the eyeball choroid through the pars plana while the sensing part remains outside the choroid and under the conjunctiva of the eye, as shown in Figure 4-5. This kind of placement is similar to that of [70].

In addition, this work also includes a designed passivation to retain the device's high quality factor. Although the sensing coil is kept outside the eyeball in this new implantation, the tissue under the conjunctiva can still cause the reduction of the quality factor induced by the tissue power absorption. To counter this, we adopted an approach of parylene-C passivation, in which enough parylene-C was deposited to contain the electric field in between different coil turns. By quantitatively measuring the effects of parylene-C passivation with different parylene-C thicknesses, the results have shown that the quality factors of the sensing coils immersed in the saline could indeed be recovered to the original values as in air. As shown in Figure 4-14, it was concluded that an extra 20 μm parylene-C passivation layer applied on top of the original sensing coil helped

maintain senor's high quality factor when it was covered by the human body tissues. Ultimately, the passivation will enable long sensing distance after the implantation.

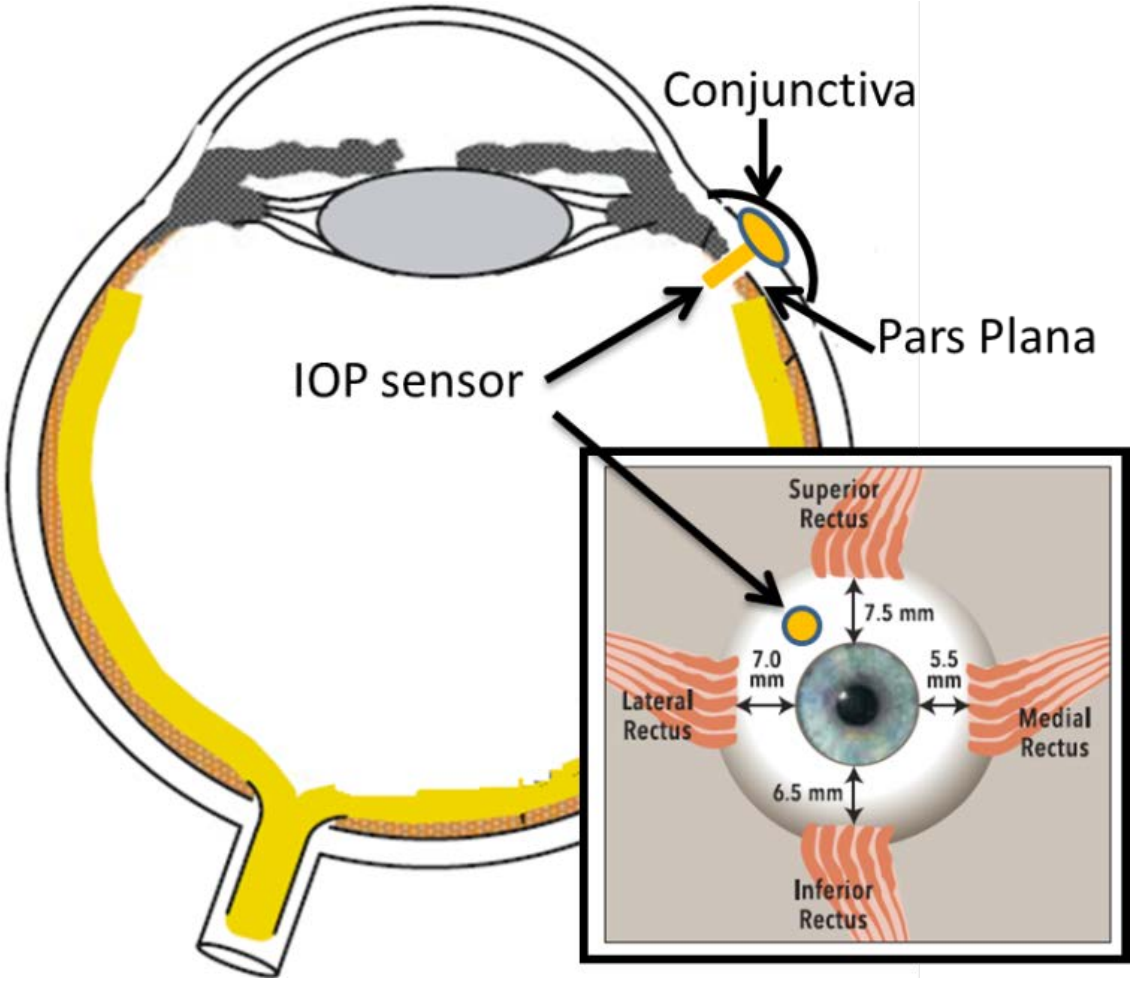

Figure 4-5: The newly designed IOP sensor is implanted at the pars plana with the implantation tube going through the choroid, while the sensing part still remains outside the choroid, but under the conjunctiva of the eye.

4.2 Sensing Theory and the Device Design

4.2.1 Sensing scheme

The wireless sensing scheme is shown in Figure 4-2. The right RLC circuit represents the implanted IOP sensor and its resonant frequency can be expressed as [97]:

$$f_s = \frac{1}{2\pi}\sqrt{\frac{1}{L_s C_s} - \frac{R_s^2}{L_s^2}} \cong \frac{1}{2\pi\sqrt{L_s C_s}} \; if \; R_s^2 \ll \frac{L_s}{C_s}, \tag{4-1}$$

where R_s, L_s, and C_s represent the sensor's resistance, inductance, and capacitance, respectively. The equivalent impedance viewed from the external coil reader and apparatus is derived as [95, 162, 165]:

$$z_{eq} = j2\pi f L_r \left[1 + k^2 \frac{\left(\frac{f}{f_s}\right)^2}{1 - \left(\frac{f}{f_s}\right)^2 + \frac{1}{Q_s} j \frac{f}{f_s}}\right], \tag{4-2}$$

where f is the excitation frequency, k is the coupling coefficient of the inductive link depending on the dimensions and separation of the coupled coils [93–95, 162, 165]. Q_s, the quality factor of the sensor at the resonance, can be represented as:

$$Q_s = \frac{1}{R_s\sqrt{L_s C_s}}. \tag{4-3}$$

When the sensor is excited at the resonant frequency, Z_{eq}, eqn. (4-2), becomes

$$Z_{eq} = j2\pi f_s L_r (1 + jk^2 Q_s), \tag{4-4}$$

and its phase dip magnitude can be approximated as:

$$\Delta\phi \cong \tan^{-1}(k^2 Q_s). \tag{4-5}$$

when the capacitance of the IOP sensor changes, it can be shown from eqns. (4-3)–(4-5). that the impedance phase dip shifts to either lower or higher frequency which can be detected by a network analyzer.

4.2.2 Electrical and mechanical design of the device

The electrical design of the IOP sensor can be explained by the well-developed equations as follows [92, 98, 166]. The inductance of the spinal coil can be represented as:

$$L_s \cong \frac{\mu_0 n^2 d_{avg} c_1}{2}\left[ln\left(\frac{c_2}{F}\right) + c_3 F + c_4 F^2\right], \tag{4-6}$$

where n is the number of turns of the inductor, d_{avg} is the averaged diameter of the coil windings, $F=(d_{out}-d_{in})/(d_{out}+d_{in})$ is the fill factor of the coil windings, and c_1-c_4 are constants determined by the winding geometry. The coil winding inherently comes with a resistance and can be calculated as:

$$R_s = \frac{\rho l}{w\delta\left(1 - e^{-h/\delta}\right)}, \tag{4-7}$$

where ρ is the electrical resistivity of the metal, w and h are the metal line width and height, respectively. δ is the frequency-dependent metal skin depth which can be written as:

$$\delta = \sqrt{\frac{\rho}{\pi f \mu}}, \tag{4-8}$$

where μ is the magnetic permeability of the metal. The capacitance of the IOP sensor is given by

$$C_s = C_{s,g} + C_{s,p}, \tag{4-9}$$

where $C_{s,g}$ is the capacitance of the parallel metal plate capacitor at the center of the IOP sensor and $C_{s,p}$ is the parasitic/stray capacitance introduced by other components in the entire device.

To have a detectable impedance phase dip shift, a deformable circular metal plate was designed at the center of the IOP sensor. Once the plate deforms either downward or upward, the capacitance of the parallel-metal-plate capacitor changes and the impedance phase dip shifts can be registered. The deformation of the metal plate corresponding to the pressure difference can be predicted as [167]:

$$w(r) = \frac{\Delta P a^4}{64D}\left[1 - \left(\frac{r}{a}\right)^2\right]^2, \tag{4-10}$$

where Δp is the pressure difference, r is the radius calculated from the center of the plate, a is the diaphragm radius and D is the flexural rigidity of the diaphragm, which is calculated as:

$$D = \frac{Et^3}{12(1-\nu^2)}, \tag{4-11}$$

where E is the Young's modulus, υ is the Poisson's ratio of the parylene-C, respectively. t is the diaphragm thickness.

In our new sensor implantation approach, the sensing metal plate deforms convexly with higher surrounding pressure transmitted to the metal diaphragm capacitor chamber through the implantation tube. According to eqn. (4-1), this higher eye pressure causes the capacitance to reduce and thus the resonant frequency shifts to the higher range, as described in Figure 4-3 (c).

4.3 Device Fabrication and Characterization

4.3.1 Device fabrication

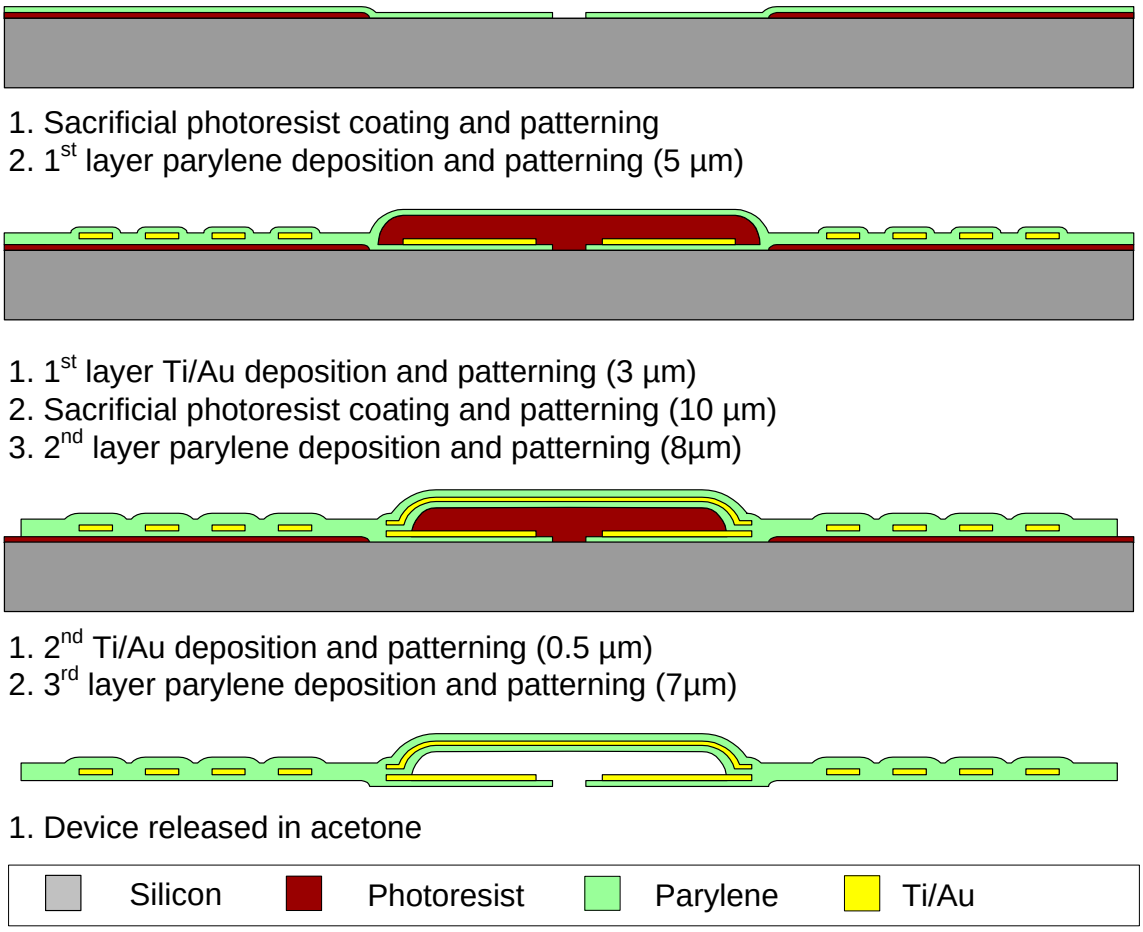

Figure 4-6: Fabrication procedures of the sensing part of the IOP sensor

The fabrication procedure of the sensing coil is shown in Figure 4-6. The sensing part was made of parylene-gold (3 µm)-parylene sandwich structure. The first layer of 5 µm parylene-C was first deposited on top of a layer of sacrificial photoresist. The pressure access hole with 180 µm in diameter was opened by oxygen plasma. 3 µm Ti/Au was deposited on top of the first layer parylene-C and patterned. The distance between two capacitor metal plates was designed as 10 µm and was achieved by spin

coating and patterning a 10-μm-thick sacrificial photoresist. A second layer of parylene-C was deposited to cover and protect the 3 μm Ti/Au; followed by a 0.5 μm Ti/Au deposition. The third parylene-C layer was then deposited and the configuration of the sensing part was patterned by oxygen plasma. The sensing part was finally released from the substrate by soaking in the acetone. The completed sensing part is shown in Figure 4-7 (a). After completing the fabrication of sensing part, the implantation tube was attached onto the backside of it, as shown in Figure 4-7 (b). The inner diameter of the implantation tube was chosen as 320 μm to fully cover the pressure access hole. The outer diameter of the implantation tube was 450 μm. The implantation tube was manually mounted onto the sensing part. A precision XYZ stage was used to control the position of the implantation tube which was maneuvered to be concentric with the pressure access hole. The implantation tube and sensing part were glued together with a few drops of biocompatible epoxy.

4.3.2 Device characterization

The completed IOP sensor was then integrated to a bigger testing capillary tube and sealed by photoresist, as shown in Figure 4-7 (c). The inner diameter of the testing tube was chosen as 500 μm to accommodate the implantation tube. The completed sensor with testing capillary tube assembly was left overnight to dry the photoresist.

The device characterization setup is shown in Figure 4-8. The whole IOP sensor assembly was mounted onto a pressure characterization setup. During the characterization, a HP 4195A network/spectrum analyzer was hooked up with a 1.5-mm-diameter hand-wound coil serving as the reader coil. The characterization signal was accessed *via* a data acquisition system and then analyzed in personal computer. The

qualified IOP sensor was released by soaking the whole assembly in the acetone to remove the photoresist. The final IOP sensor is shown in Figure 4-7(d) and is ready for the next *in vivo/ex vivo* test.

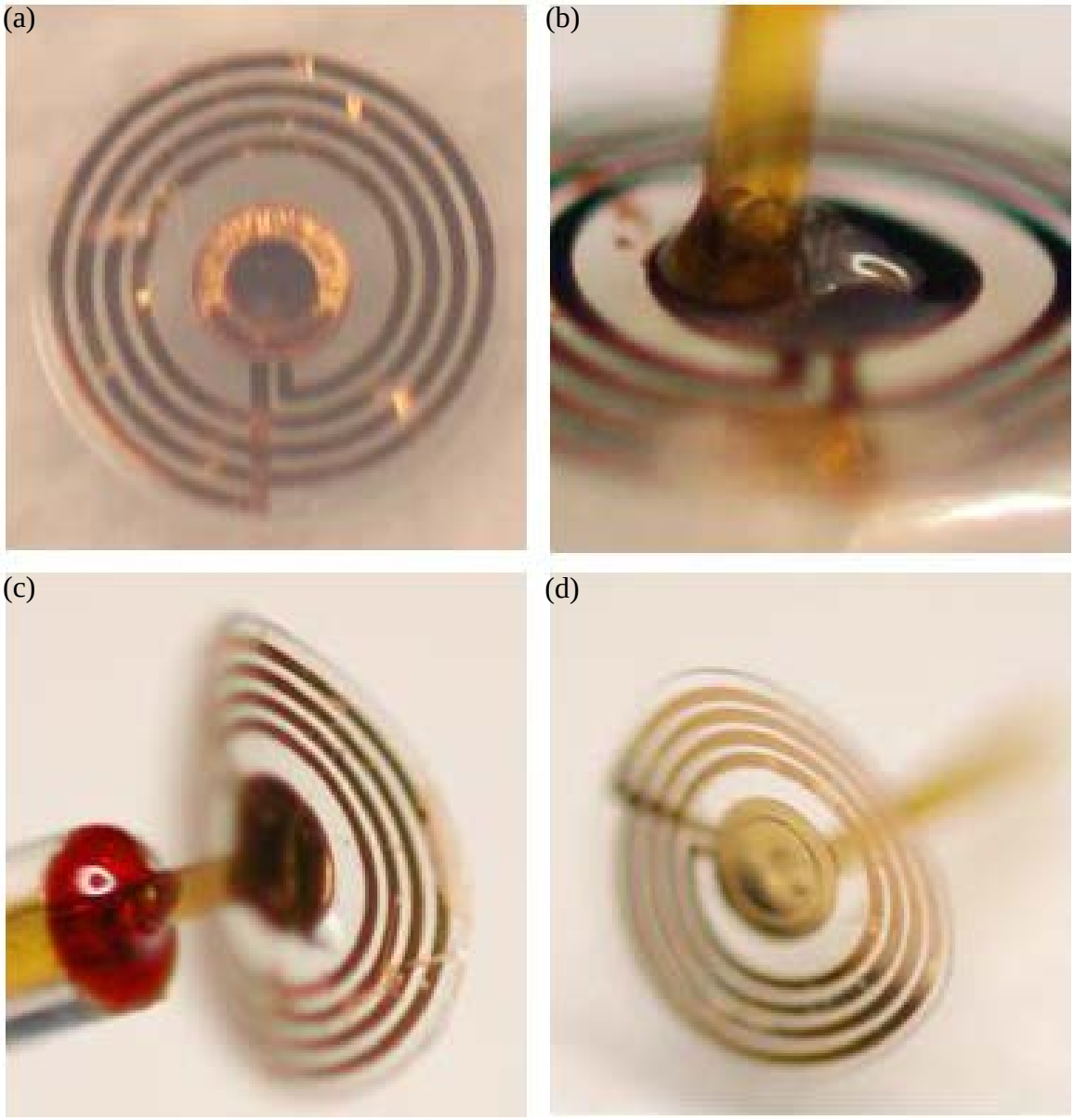

Figure 4-7: IOP sensor fabrication and assembling results: (a) Completed sensing part, (b) implantation tube attached onto the backside of the sensing part concentric with the pressure access hole, (c) IOP sensor mounted to the testing tube by photoresist, (d) final IOP sensor

4.4 Characterization Results and Discussions

The benchtop characterization results are shown in Figure 4-9. The results show that the resonant frequency was 379 MHz when the applied pressure difference was 0 mmHg. When the applied pressure difference increased, the resonant frequency shifted to the right as expected because the metal plate deformed convexly. The IOP sensor's electrical parameters were obtained and shown in Table 4-1.

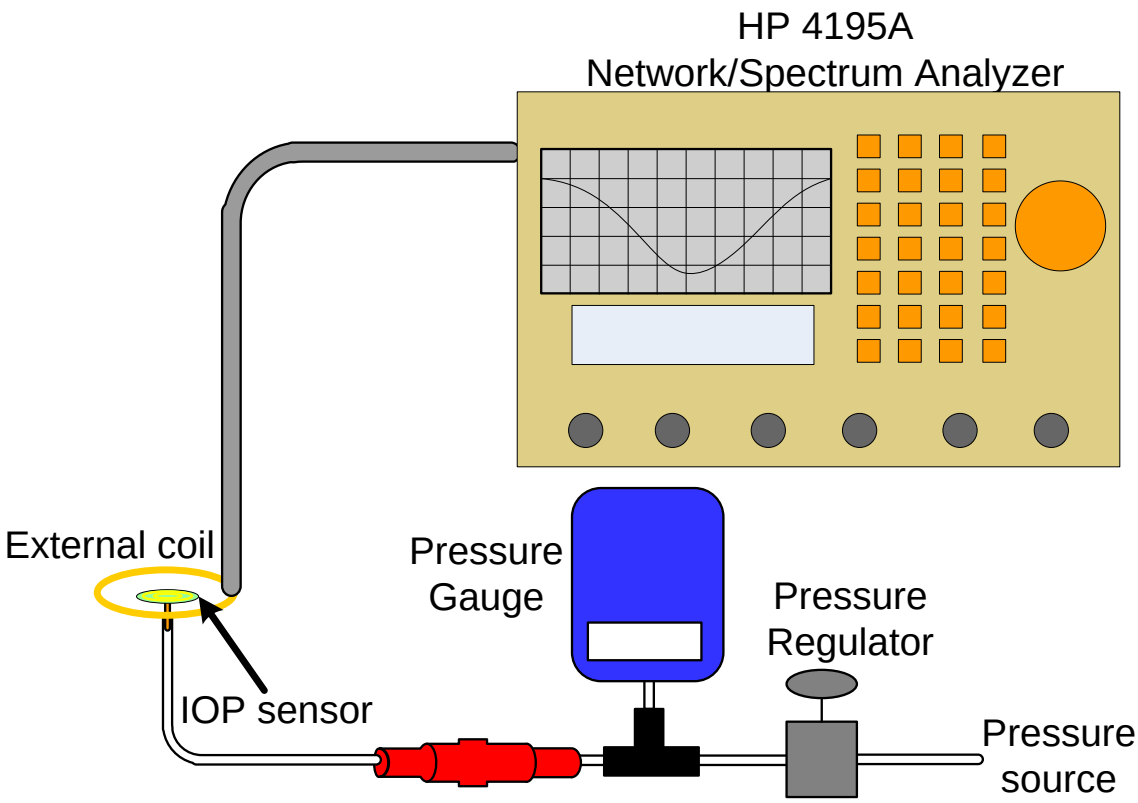

Figure 4-8: IOP sensor characterization setup: a 1.5-mm-diameter hand-wound coil served as the reader coil and a HP4195A network/spectrum analyzer was used to register the frequency shift of the phase dip.

Table 4-1: Dimension of the new IOP sensor and its measured electrical parameters

Planar dimension	4 mm (foldable)					
Pressure (mmHg)	0	20	40	60	80	100
Frequency (MHz)	379	381	385	390	395	402
Q Factor	27	27	28	30	28	29
Sensitivity	542 ppm/mmHg					
Responsivity	205 kHz/mmHg					
Sensing distance	2.5 cm					

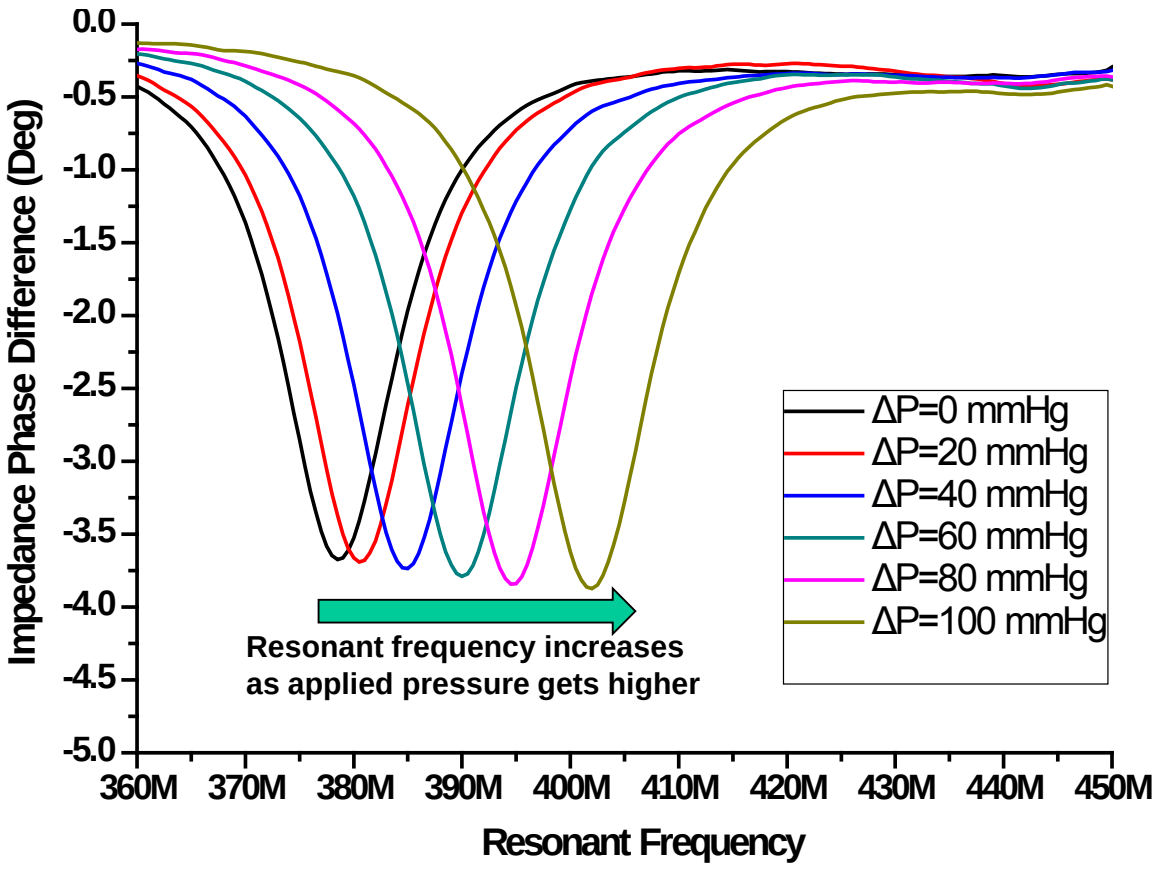

Figure 4-9: Bench-top characterization results of the IOP sensor: the resonant frequency was 379 MHz when the applied pressure difference was 0 mmHg, and shifted to higher frequency when the pressure difference increased.

As the sensing part can always be maintained exposed outside the anterior chamber, the quality factor drop caused by the lossy medium is largely alleviated in this work. Therefore, the new implant possesses farther sensing distance than the one implanted right in the anterior chamber, which was originally designed to have 2.5 cm sensing distance. The new design enables a glass reader paradigm to accomplish the autonomous, continuous, and wireless IOP monitoring.

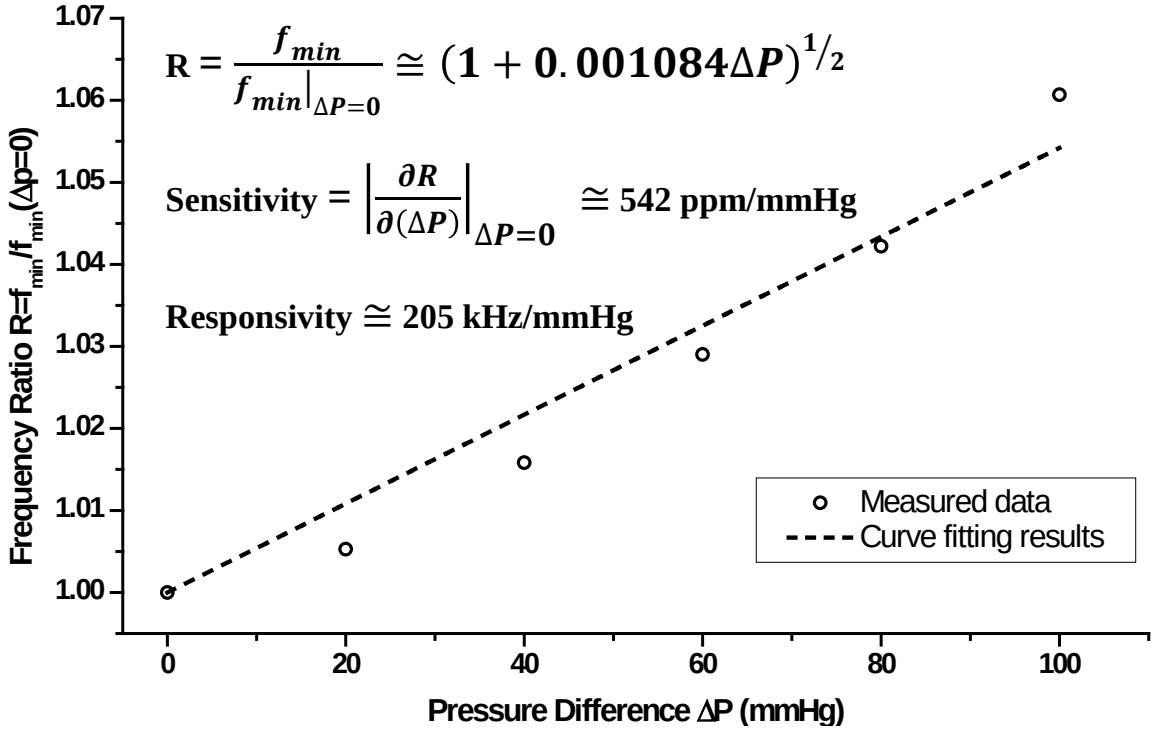

Figure 4-10: Sensitivity analysis of the IOP sensor

The result of sensitivity analysis is shown Figure 4-10. The sensitivity of the IOP sensor is defined as [97]:

$$\text{IOP sensor sensitivity} = \left|\frac{\partial R}{\partial(\Delta P)}\right|_{\Delta P=0}, \tag{4-12}$$

where *R* is the frequency ratio defined as:

$$R = \frac{f_{min}}{f_{\min(\Delta P=0)}}. \quad (4\text{-}13)$$

A sensitivity of 542 ppm/mmHg was obtained for the IOP sensor, corresponding to the responsivity as 205 kHz/mmHg. With a proper designed high resolution external coil reader, the IOP sensor can resolve the pressure difference < 1 mmHg, which is suitable for glaucoma diagnostics.

4.5 Quality Factor Recovery Study

4.5.1 Overview

As mentioned in [98], the quality factor of the transmitting coil, i.e. transmitting resonant tank, dropped a lot (from ~ 30 down to ~ 6) when implanted in the anterior chamber, which resulted in a great reduction of the sensing distance (from 2.5 cm to 1.5 cm). As the loss tangent represents the power loss in the medium, this quality factor drop is due to the high loss tangent of the eye fluid in the anterior chamber. For lossy medium such as saline, the permittivity, $\boldsymbol{\varepsilon}$, can be written in the complex form as [168–170]:

$$\varepsilon = \varepsilon' - j\varepsilon'', \quad (4\text{-}14)$$

with the loss tangent defined as:

$$\text{loss tangent} = \frac{\varepsilon''}{\varepsilon'} \quad (4\text{-}15)$$

which represents the power loss in the medium. The loss tangent value of saline is reported as about 0.2 [95, 169], which is much higher than of the air, and close to that of body tissue and eye fluid. This means the electromagnetic energy of the IOP sensor dissipates more easily in the anterior chamber. Although in our work, only the implantation tube penetrates into the eyeball and leaves the sensing part under the conjunctiva, the quality factor can still drop due to the covering human body tissues.

4.5.2 Q factor recovery by passivation layers of different materials

Except for modifying the implantation scheme as depicted in Section 4.2, another way to solve the problem is to try to strengthen the isolation between the sensor structure and the surrounding medium [95, 97]. In this section, three different materials: regular glass cover slip, photoresist, and regular 5 min epoxy, are used to cover the IOP sensors as the passivation layers to isolate the devices and the surrounding medium. The loss tangents of these covering materials are expected to be lower than the saline, and hence could improve the quality factor when the devices are immersed in the saline.

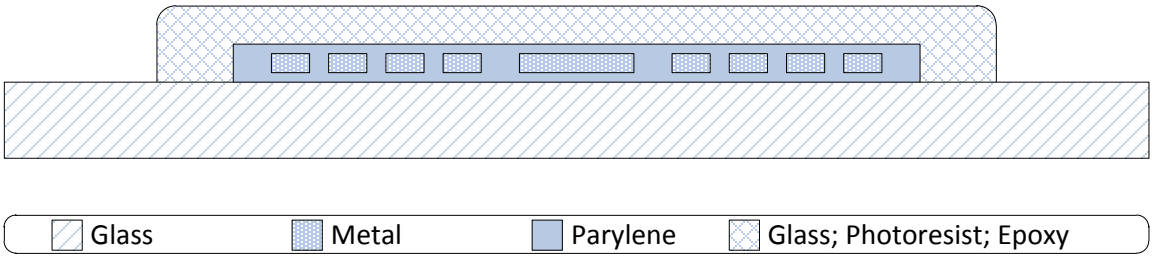

Figure 4-11: The idea of covering the device with different passivation layers: glass cover slip, photoresist, or epoxy. The IOP sensor is shown in gray in the figure.

The idea of covering the devices with passivation layers is shown in Figure 4-11. These testing samples as shown in light blue were first placed on top of the glass cover slips and characterized in the air before they were covered by the passivation layers. Only one passivation layer was then applied to the top of the device and the entire device was characterized again. Two examples of the completed devices are shown in Figure 4-12. The completed devices were tested both in the air and saline to study the efficiency of the covering of the passivation layers. For photoresist as the passivation layer, a

second layer of photoresist was painted on top of the first photoresist layer again followed by the same quality factor characterization procedures to study the thickness effects of the photoresist passivation layers.

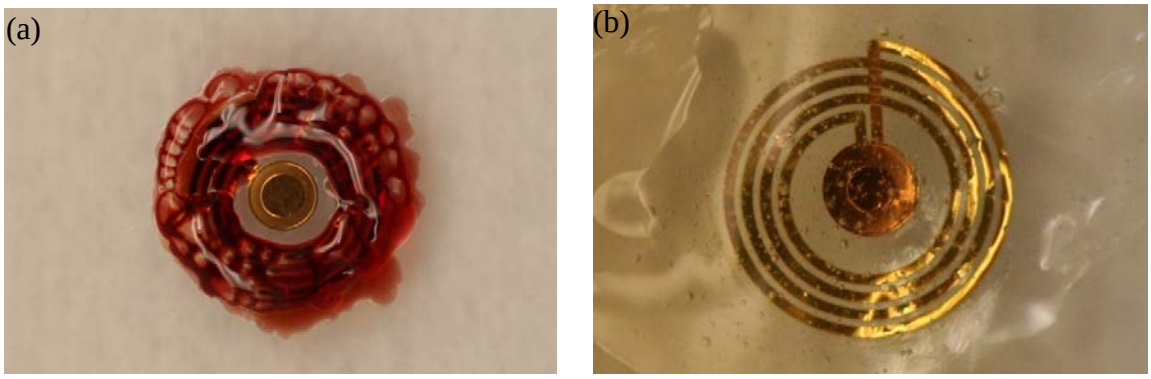

Figure 4-12: IOP sensors covered by two different materials with low loss tangent: (a) photoresist and (b) epoxy

The diameter of the reader coil was about 11 mm and the sensing distance was about 9 mm. The characterization results are shown in Table 4-2. The first device sample was covered by a regular glass cover slip with 0.2 mm in thickness. Sample 2 and 3 shared the same treatment of photoresist passivation layers. Sample 4 was covered by the regular 5-min dry epoxy. The results show that the quality factors of the original devices fell in the range of 23.6–28.76, and dropped from 23.6 measured in the air to 2.69 measured in the saline without any passivation layer (Sample 4).

For the device covered by the cover slip (Sample 1), however, the Q factor was kept almost unchanged and the Q factor was maintained at 15.74. For the two devices covered by the photoresist (Sample 2 and 3), the Q factors dropped from 28.76 (Sample 2) and 27.13 (Sample 3) to 25.37 (Sample 2) and 22.5 (Sample 3) when devices were exposed to the air. Furthermore, the Q factors of Sample 2 and Sample 3 dropped to 4.11

(Sample 2) and 5.07 (Sample 3) when the devices were immersed in the saline. The thickness of one layer of the photoresist was measured about 45 μm. To study the thickness effect of the photoresist passivation layer, another layer of the same type of photoresist was painted on the device again. When the devices were exposed to the air, the obtained Q factors were recovered from 25.37 (Sample 2) and 22.5 (Sample 3) to 25.98 (Sample 2) and 29.48 (Sample 3). When the devices were immersed in the saline, the improvements of the obtained Q factors were more obvious: 4.11 to 10.54 (Sample 2) and 5.07 to 8.98 (Sample 3). Sample 4 was covered by regular 5-min dry epoxy and the result showed that the Q factor dropped from 23.6 to 18.84 (in the air) and 11.49 (in the saline).

Table 4-2: Measured quality factors with different isolation layers covered on top

	Sample 1	**Sample 2**	**Sample 3**	**Sample 4**
No isolation layer Tested in the air	25.47	28.76	27.13	23.6
Isolation layer	Glass cover slip	One side PR	One side PR	---
Isolation layer thickness	---	~ 45 μm	~ 45 μm	---
In the air	24.43	25.37	22.5	23.6
In saline	15.74	4.11	5.07	2.69
2nd isolation layer	----	PR paint again	PR paint again	Epoxy
2nd isolation layer thickness	----	~ 90 μm	~ 90 μm	NA
In the air	----	25.98	29.48	18.84
In saline	----	10.54	8.98	11.49

In summary, it is observed that, when the device is exposed to the air, the measured Q factor has very little change no matter what kind the passivation layer covered on top. In terms of the device characterization in the saline, the Q factors are always smaller than its original values even with the passivation layers. Even though, the characterization results still show that the passivation layers do preserve the Q factors after the passivation layers covering. Among all of the three passivation materials, the glass cover slip demonstrates the best restoring result according to Table 4-2. One of the reasons is because of its high thickness (0.2 mm). The thickness effect of the photoresist passivation layer is very obvious.

On the other hand, the isolation efficiency of the epoxy seems to be better than photoresist when the characterization is performed in the saline, but not in the air. It is likely attributed to the epoxy thickness is much higher than photoresist so that the coil is more effectively isolated from the saline. However, the isolation efficiency of the epoxy for device characterized in the air is not as good as others. It is also found that the two Q factors obtained of sample 4 (both in the air and in saline) are closer in comparison to other passivation materials. The assumption is that the loss tangent of the epoxy is higher than the photoresist, causing a lower Q factor when measured in the air. However, the higher epoxy thickness can more effectively isolate the device from the saline solution, and hence results in a higher Q factor than covered by photoresist.

4.5.3 Q factor recovery by parylene-C passivation layers

Section 4.5.2 has successfully demonstrated the concept of recovering the Q factor to a certain level by covering the devices with passivation layers. However, those materials used in Section 4.5.2 are either not flexible enough (glass cover slip) or not

biocompatible at all (photoresist and 5-min-dry epoxy). In order to recover the device's Q factor while still preserving its biocompatibility, a material needs to not only have a low loss tangent, but also to be flexible and biocompatible.

In addition to its superior flexibility and biocompatibility, parylene-C is also compatible with the most of the surface micromachining fabrication procedures and hence has very good machinability. Furthermore, parylene-C is found to have loss tangent with 0.1 [171], which is much lower than saline (0.2), implying that it can be a very good candidate for the passivation layers described in Section 4.5.2. Therefore, to restore the high quality factor, quantitative investigation has also been done by putting multi-layer parylene-C films on top of the sensing coil to regain its quality factor when it is submersed in the saline.

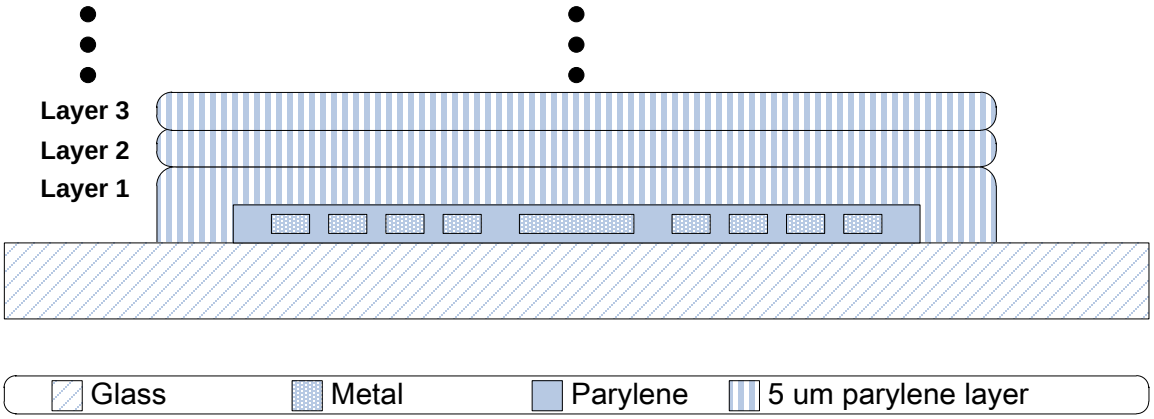

Figure 4-13: The idea of covering the device with several layers of parylene-C sheets. The IOP sensor is shown in gray in the figure.

The concept of the experiment is shown in Figure 4-13. An original sensing coil with the 7 μm parylene-C deposited on top was first mounted onto a glass slide. Multiple 5-μm-thick parylene-C films were put on top of the sensing coil layer by layer until 40

μm parylene-C accumulated. Every time before the next 5 μm parylene-C film was put on, the coil was characterized both exposed in the air and also submersed in the saline. The quality factors were calculated to investigate the quality factor recovery capability with respect to different parylene-C thicknesses.

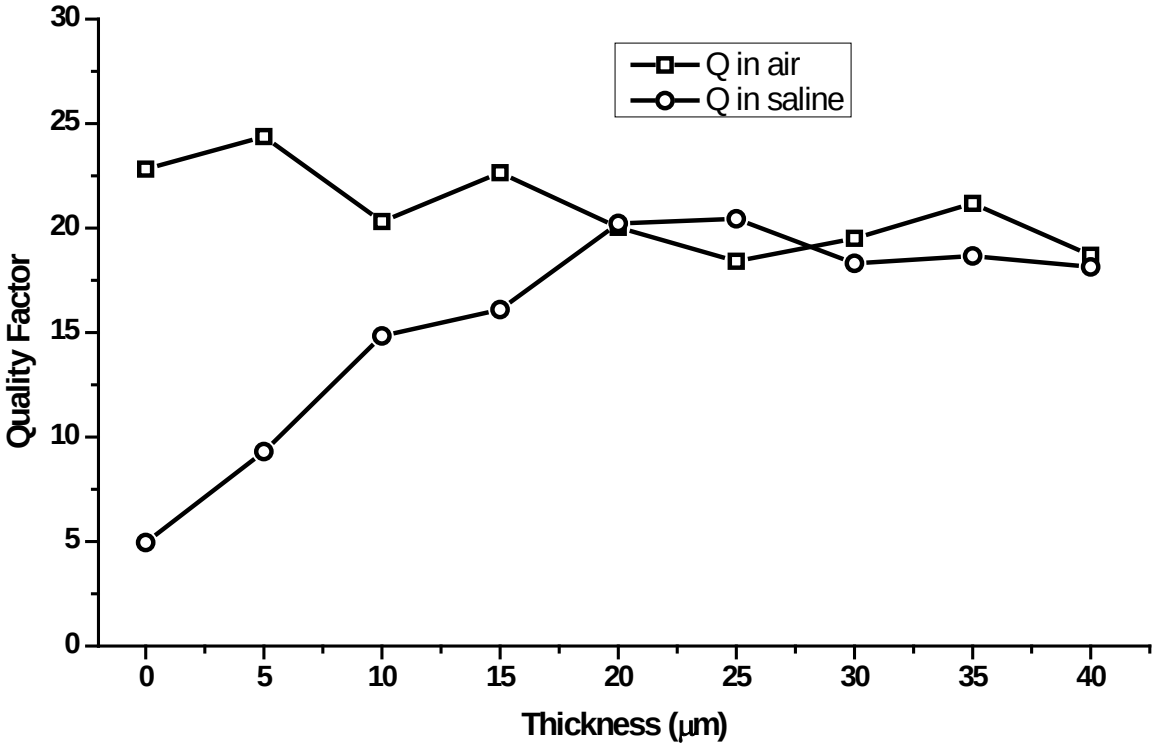

Figure 4-14: Quality factor recovering results versus parylene-C thickness by covering the IOP sensor with several parylene-C layers

The sensor's quality factor measuring result versus the parylene-C layer thickness is shown in Figure 4-14. When only 7-μm-thick parylene-C covered on top of the sensing coil (the original sensing coil), the quality factor was measured only 4.95 in saline while it was measured as 22.83 in the air. The obtained quality factors (in saline) increased with the increasing parylene-C thicknesses, and saturates at about 17–20 when

the parylene-C thickness reached 20 μm. In other words, the Q factor measured with the device immersed in the saline was noticeably recovered. As the recovered Q factor (device immersed in saline) reached the same level as the Q factor (device exposed to the air) when the parylene-C thickness reached 20 μm, we concluded that the sensing coil would not be affected by the surrounding saline when the thickness of the covering parylene-C layer reached 27 (20+7) μm. It is therefore proved that a 30-μm-thick parylene-C passivation layer is sufficiently thick to be deposited on top of the metal coil.

It is also found that the quality factor measured with the device exposed in the air dropped a bit from 22.82 to ~ 20 as the parylene-C passivation layer increases. This is likely attributed to the fact that the loss tangent of the parylene-C, 0.1, is still higher than the air.

4.5.4 Summary

In summary, it is found that the Q factor can be recovered by covering the devices with at least extra 20 μm parylene-C passivation layers. Theoretically, 20 μm parylene-C can be easily created by standard parylene-C deposition process and then patterned by oxygen plasma. It needs to be noted that, however, during the parylene-C deposition, 20-μm-thick parylene-C would also deposit onto the metal plates of the parallel metal-plates capacitor. This would increase the parylene-C thickness of the deformable plate, resulting in the loss of the capacitor sensitivity. To overcome this problem, one more process with oxygen plasma etching could be used to thin down the parylene-C layer right on top of the metal-plate capacitor, as demonstrated in Figure 4-15.

4.6 Summary and Conclusion

In this chapter, we have successfully demonstrated the feasibility of the new concept and design of the IOP sensor implant. A parylene-C-based sensing part with about 30 µm in overall thickness was first fabricated, and then integrated with an implantation tube attached to the sensor's backside pressure access hole.

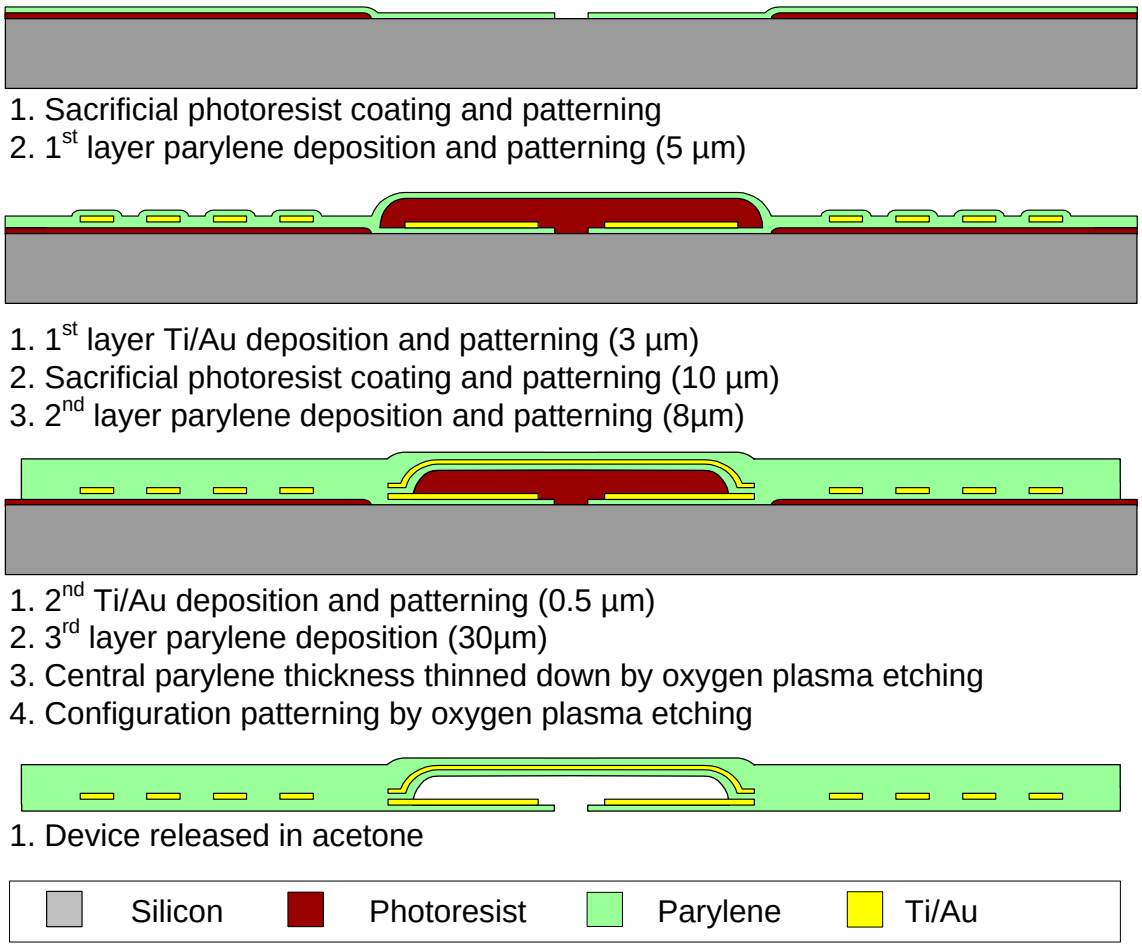

Figure 4-15: Modified sensing coil fabrication procedures: After 30 µm parylene-C layer is deposited on top of the capacitor metal plate, an extra oxygen plasma etching process is executed to thin down the central parylene-C to retain the capacitor sensitivity.

A new surgical placement of the device was also proposed. The new IOP sensor was implanted at the pars plana with the implantation tube penetrating through the choroid, while the sensing part still remained outside the eyeball but covered by the conjunctiva. Without the influence of the surrounding aqueous humor, this implantation approach can maintain the high quality factor of the device and thus a 2.5 cm sensing distance can be fulfilled. This enables the glass reader paradigm concept, and therefore achieves autonomous, continuous and wireless IOP monitoring.

The sensitivity was obtained as high as 542 ppm/mmHg while the responsivity was about 205 kHz/mmHg. The characterized IOP sensor is ready for use, and the *ex vivo*/ *in vivo* test can be scheduled in the near future to verify the biological feasibility. In addition, the future work would also focus on the fixation of the IOP sensor. The possible solution would include enlarging the parylene-C area of the sensing coil of the device, enabling the possible suturing of the parylene-C sensing part.

Besides, the quality factor can be recovered also by covering the device by low loss tangent materials as passivation layers to isolate the device and the saline. It is found in Section 4.5 that parylene-C is a very good passivation layer to recover the Q factor due to its low loss tangent. Experimental results showed that the Q factor was mostly recovered by an extra 20 μm parylene-C film. We demonstrated that a 30-μm-thick parylene-C on the capacitor metal plate could maintain the sensor's high quality factor in saline or under human tissue.

Furthermore, parylene-C isolation layer can also be easily achieved by standard parylene-C deposition process, followed by oxygen plasma etching to remove the excess parylene-C on top of the capacitor to maintain the sensitivity of the IOP sensor.